1996

Development of a Comprehensive Thermodynamic Modeling System for Refrigerant Screw Compressors

J. Sauls
The Trane Company

Development of a Comprehensive Thermodynamic Modeling System for Refrigerant Screw Compressors

Jack Sauls, Staff Engineer
Trane Company Engineering Technology, La Crosse, WI 54601

Abstract

This paper describes analytical and experimental efforts leading to a complete thermodynamic simulation of refrigerant screw compressors with emphasis on methods for inspection of experimental compressors and assembly analysis to determine actual clearances for specific test compressor. This work led to a better understanding of leakage and improved analysis in the thermodynamic model. The need for accurate modeling of all of the compressor components is also discussed, with brief descriptions of the models used provided.

Introduction

There have been many thermodynamic modeling systems for screw compressors (see /1/ and /2/). The thermodynamic analysis in the system described here shares characteristics with many of these. However, the model contains a collection of elements in addition to the compression simulation. The design system also includes comprehensive assembly analysis procedures which provide important clearance information to the simulation.

A schematic of the system in Figure 1 shows the two main elements, a thermodynamic simulation and an assembly model. Both branches use generic solvers. The thermodynamic solver is used in a scroll compressor simulation and the assembly solver is used in assembly analysis and design programs.

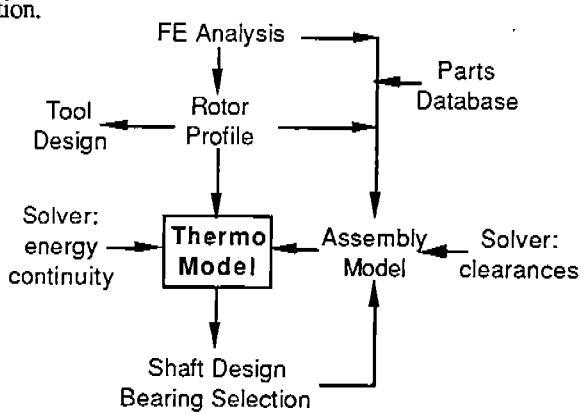

Figure 1
Screw Compressor Modeling System

A detailed analysis of compression within the screw rotors is included in a broader simulation of a complete compressor where effects such as motor loss, pressure losses and liquid or vapor injection are added. The model also includes a cycle analysis. Separate programs supply rotor geomety data and shaft and housing deflections for clearance calculations. The compressor model programs provide geometric and gas load data to rotor profile tool design, shaft design and bearing selection programs.

Clearances are an important part of the simulation. A branch of the modeling system has been set up to provide analysis of assembled clearances. A database of information from measurements of critical parts is used to compute internal clearances. The procedure can include the effects of thermal and pressure loads, providing an accurate picture of the clearances in the running compressor. This information is important in interpreting test data and using it to improve the simulation model.

Thermodynamic Model

The thermodynamic model has three elements — modeling compression within the rotor pair, modeling the compressor containing the rotors and modeling the cycle with the compressor. The compression process is represented by real gas forms of the energy and continuity equations with explicit treatment of individual mass and heat flows. The resulting set of differential equations are solved as an initial value problem. The initial state in the rotors is dependent on suction side pressure losses and hermetic motor losses which are in turn affected by the mass flow and power characteristics of the rotors. An extended model includes analysis of these and other elements of overall compressor performance. In addition, an embedded cycle calculation provides a consistent solution for mass flow rates and pressures for economizer cycles and unloaded operation with relief.

Compression process modeling can be carried out for a variety rotor geometries, discharge port options, rotor and housing clearances and oil and/or liquid refrigerant injection. Clearance options include variations in rotor-to-housing clearance as a function of position within the housing, variation in rotor-to-rotor clearance along the length of the rotor, separate rotor-to-slide valve clearances and separate rotor discharge end clearances. Porting options include separate radial and axial discharge ports with geometries computed based on specified volume ratio and automatic adjustment of radial port geometry for slide valve unloader geometry. Options for four mechanical unloader configurations are provided, including details such as 'clearance volumes' for piston type ports which do not close flush with the housing.

Other elements included in the full model are: constant or variable speed open or hermetic motor performance; inlet and discharge pressure losses based on specified geometry; unloader gallery loss based on gallery geometry; discharge pulsation with

interaction with compression during discharge; calculated refrigerant concentration in oil at computed oil separator conditions and inclusion of this effect in the compression solution; high-to-low side heat transfer based on specified geometry and solution parameters; automatic solution for cycle saturation temperatures for part load analysis of operation in a system with head relief; and calculation of leakages through various shaft and cavity seals, including thrust balance pistons. The program manages the interaction between the compression process model and the collection of extra effects that define the complete simulation.

Internal Leakage

Leakage through internal clearances is a major determinant of screw compressor performance. These flows are affected by moving boundaries, complex and varying flowpath geometries and the presence of oil. Leak path pressure ratios range from very low to well beyond critical and there is a wide range in Reynold's number. This nearly overwhelming complexity is often modeled as a simple nozzle flow, modified by estimated or empirically determined coefficients. This is the case for the model reported here. Figure 2 shows rotor-to-housing and rotor-to-rotor leak locations with the corresponding simple nozzle representation for flow calculations. The flow rate, $\dot{m}$, is computed from:

$$\dot{m} = \rho_t \cdot V_t \cdot \Psi \cdot \text{Area} \qquad (1)$$

Velocity V_t and density r_t are determined for real gas, which may be an assumed homogeneous oil/refrigerant mixture, using equations (2) and (3). If the flow is not choked, the throat static pressure is the low pressure side pressure ($p_t = p_2$) and the entropy and stagnation enthalpy are the same as the source chamber ($s_t = s_1$ and $h_{0t} = h_1$):

$$h_t = f(p_t, s_t) \quad \text{and} \quad \rho_t = f(p_t, s_t) \qquad (2)$$

$$V_t = \sqrt{2 \cdot (h_{0t} - h_t)} \qquad (3)$$

If the flow is choked, the throat velocity is the local speed of sound.

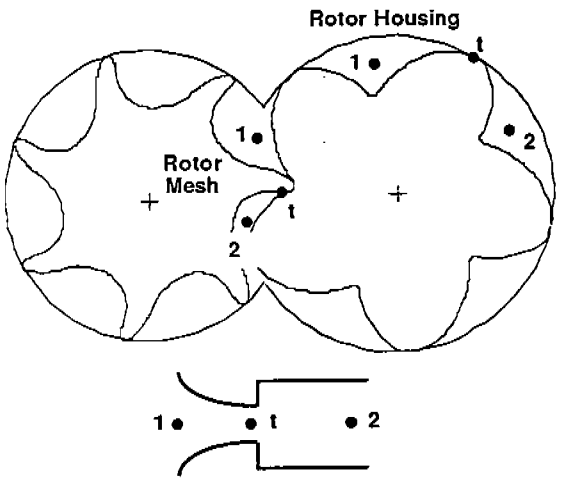

Figure 2
Leak paths and Flow Model

There are many issues to be considered in using this simple model and most have received attention in the literature. Two factors are covered here—the flow coefficient Ψ and the leakage area. Any model is improved with experience with actual compressors. Comparing predictions with tests allows calibration for unknown factors such as defined by $\Psi \cdot \text{Area}$ in equation (1). This is best done if the area is known so geometric factors do not become part of the flow coefficient. The next section describes how clearances for compressors built and tested to measure performance characteristics are determined.

Assembled Clearances

A computer assisted screw compressor clearance analysis and build documentation procedure /3/ is used to determine assembled clearances using measured dimensions of actual parts or drawing data. Both cold (as assembled) and hot (as running) clearances are calculated and a complete build summary of each compressor is printed. Drawing data and data from inspections of critical parts is linked to a Microsoft EXCEL™ "assembly log" workbook, which can compute clearances, generate clearance charts and write a summary. Rotor-to-housing, rotor-to-slide valve and rotor intermesh clearances are computed under the influence of the following:

- Bearing clearance, rotating eccentricity and stationary eccentricity
- Rotor and bearing deflection due to gas loading
- Slide valve rotation due to key and key slot width differences and slide valve in running or static position in bore.
- Dowel pin eccentricity (for clearance adjustments).

Use of the assembly log during an experimental program offers the following advantages:

- Analysis of effects of alternative part selections on clearances
- Identification of reliability or performance threatening clearance situations before running the compressor
- Rapid analysis of effects of reworking parts to improve reliability or performance
- Complete documentation of selected build geometry

Three main parts — the rotor housing, discharge bearing housing and slide valve unloader — are checked on a coordinate measuring machine (CMM). The rotor shaft is checked and the rotor profile intermesh clearance and backlash are measured. Finally, bearing under-roller diameter and other measurements are taken during assembly. All data is transferred to the database files in the assembly log program. At assembly, serial numbers for each part are entered in a data form along with measurements

obtained during the build. The form is read into the assembly log, which then gets data for the parts from the database. When all data is loaded, the built-in calculations generate a complete analysis of the particular collection of parts selected.

Figures 3 and 4 show measurement points and the general coordinate system. U-T and W-V are arbitrary axes for the CMM inspection of the male and female rotor bores. U and W locate the inlet end bearings; T and V are at the theoretical centers of the bores at the discharge end. G and F are measured discharge end bearing centers. x, y coordinates at planes N, P, R and S define bore surfaces. Bearing clearance is added at U, G, W and F to locate the shaft and bearing deflection is added for under-load analysis. Measured rotor diameters are distributed along the axis of the rotor shaft (U' G' for the male and W' F' for the female...see Figure 4).

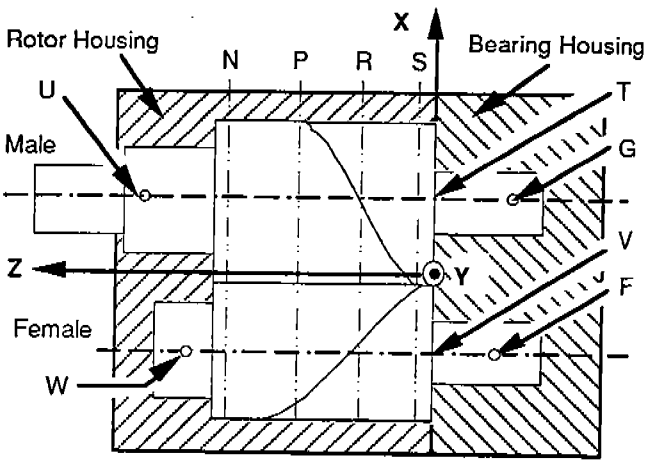

Figure 3
CMM Housing Measurements

Coordinate systems Q (Figure 4) and L exist for each measurement plane. L lies on the housing measurement axis and Q on the rotor axis. These differ from the each other because: 1) the discharge bearing G is not on measurement axis T due to offset of the bearing housing by design and from manufacturing variation; 2) the rotor axis shifts in the bearing clearance; 3) for a running compressor, the shaft moves due to bearing deflection and the axis shifts due to shaft bending.

Rotor-to-housing clearance is calculated at each measured housing point. There are typically six points on each bore at each measurement plane for a total of 24 bore coordinates. All housing coordinates are transformed into the Q coordinate system. Clearance is then the difference in the local rotor radius and the distance from Q to the transformed coordinates x,y.

L Local housing coordinates
Q Local rotor axis coordinates

Subscripts
k - measurement plane
i - measurement point

$$x'_{k,i} = x_{k,i} + X_{L,k} - X_{Q,k}$$

$$y'_{k,i} = y_{k,i} + Y_{L,k} - Y_{Q,k}$$

$$D_k' = D_k + \text{eccentricity}_k \qquad (4)$$

$$CLR_{k,i} = \sqrt{x'^2_{k,i} + y'^2_{k,i}} - \frac{D'_k}{2}$$

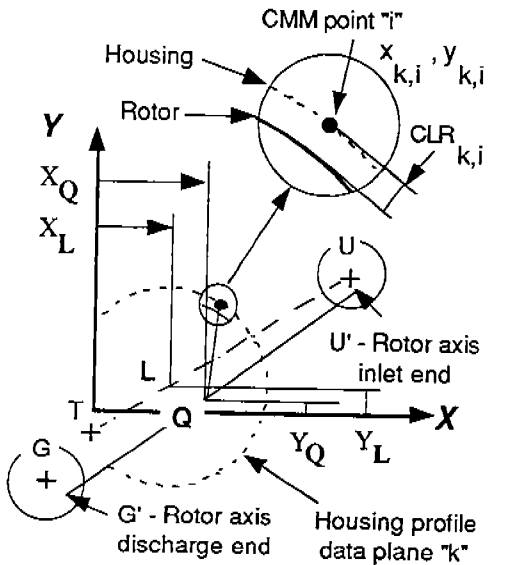

Figure 4
Coordinate Systems and Radial Clearance Calculations (Male Rotor Side)

Transformations and clearance calculations applied to a point on the male rotor housing are defined in equations (4). Coordinates measured in the L coordinate system (x, y) are transformed to the Q coordinate system (x', y'). D' is the rotor diameter plus eccentricity and defines the envelope within which the rotor rotates. Origins of the L and Q systems are defined relative to a global coordinate system *(X,Y)* defined by rotor housing dowel pin locations.

Figure 5 shows computed clearances for a 164 mm compressor. Clearances are shown for both the compressor as assembled (no thermal or bending effects included) and as run (with housing and rotor thermal distortion, shaft bending and bearing deflection). The inner arcs represent the rotors and the data represents locations of the housing bores and slide valve surfaces. The short lines pointing away from the outer grid lines show the direction of the average gas loads.

In addition to radial clearances, the assembly log computes average rotor mesh clearance. Data for the selected rotor pair is retrieved from the database and the measured mesh clearance is adjusted to the actual center distance of the build.

The assembly log thus provides a detailed picture of the clearances in a compressor. A project was initiated to systematically vary clearances in a 164mm screw compressor to determine the effect of the separate clearances and to provide data for calibration of the leakage flow models. Average radial clearances were adjusted by changing the rotor diameters. Distribution of

radial clearances for a given rotor and housing pair was also varied by repositioning the rotors relative to the housing using eccentric dowel pins. Rotor mesh clearances were varied by changing center distance. Rotor discharge end axial clearances could be set at selected levels for any configuration. A complete assembly analysis was acquired for every configuration tested in a project initiated to document the clearance effect in a 164mm screw. Test results are given in Figures 6 and 7. Figure 6 shows sensitivity to radial clearances. Analysis of the data showed that the radial clearance effect was best described with a 'representative' clearance, defined as the average of clearances for all measured slide valve points (typically 18 points) and the male and female side housing clearances at the discharge end on the high pressure side, shown in Figure 5 as clr_tm and clr_tf. The average clearance (average bore radius - average rotor radius) had little impact within the range of clearances expected based on manufacturing tolerances—positioning, not size, was the key factor. Figure 6 shows that the radial clearance affects adiabatic efficiency but not volumetric efficiency.

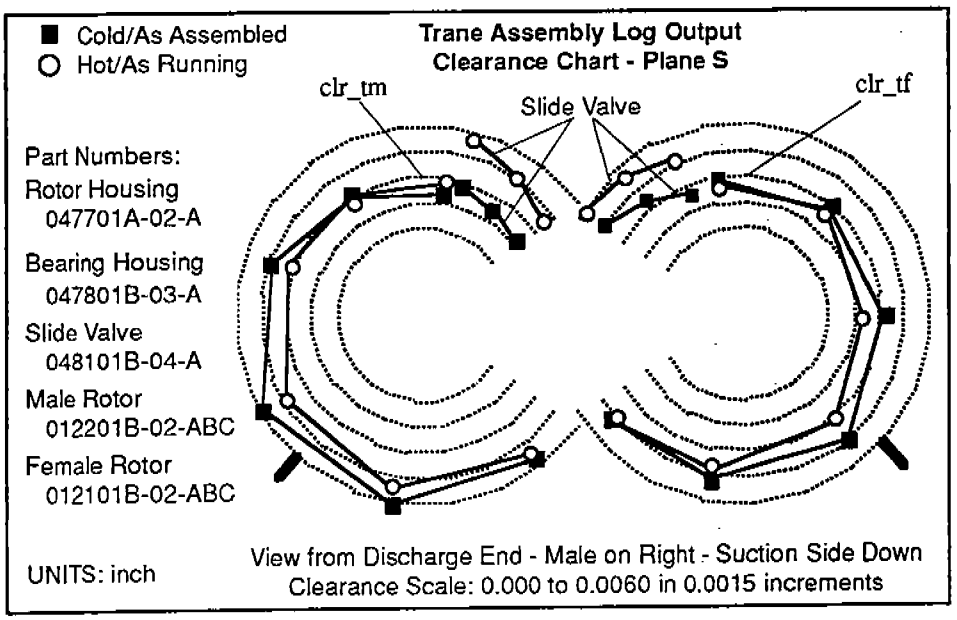

Figure 5
Clearance Analysis Chart from Assembly Log Program

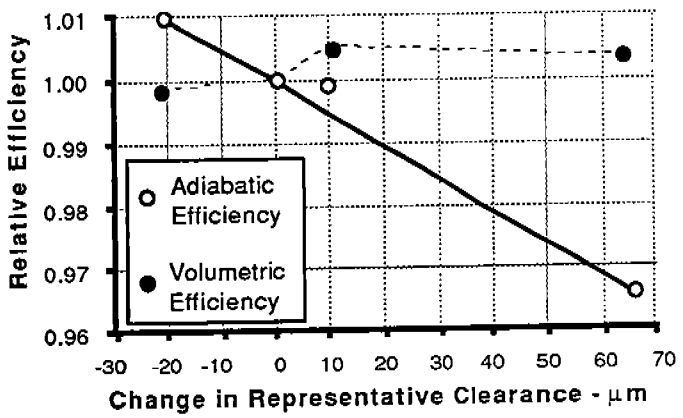

Figure 6
Effect of Radial Clearance on Performance

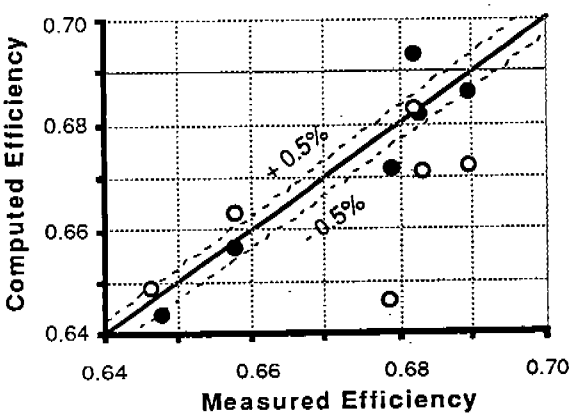

Figure 7
Simulation Improvement

The tests were also used to improve the compressor simulation. Figure 7 shows a comparison of measured and computed efficiencies for the original constant flow coefficients and a modified variable Ψ case, based on an approach suggested by Peveling's work /4/. Peveling showed that the flow coefficient was dependent on the shape of the leak path, the clearance and the Reynold's number. Using a global Reynold's number based on total mass flow and average clearance, selecting shapes for rotor-to-housing and rotor mesh and scaling Peveling's data to the test compressor design point resulted in a variable flow coefficient model. Ψ is then dependent on assembled clearance and the operating condition (affecting Reynold's number and clearances). The new model used Ψ for the rotor mesh leakage based on gap configuration 21 from /4/. The mesh Ψ varied from 0.75 at high pressure ratio (higher clearances due to load and higher leakages result in high Reynold's number), to around 0.6 at lower loads. Ψ for radial clearances was based on configuration 4 from /4/ and varied in the range from 0.8 to 1. Comparisons in Figure 7 represent several compressor builds and operating conditions. With the original constant flow coefficient ($\Psi = 1$ in all cases), the average deviation from tested performance is 1.8%. This improves to an average deviation of 0.7% with the simple variable Ψ model.

This work resulted in a strategy for specifying Ψ that can be transported with some confidence to configurations that are considerably different than the calibration compressor, since the coefficient, while calibrated, is expressed in terms of fundamental parameters such as Reynold's number and, with use of the assembly analysis, can be assumed to be relatively free of calibration for specific geometry effects.

Inlet and Discharge Pressure Loss and Pulsation

A good simulation of the compression process is the heart of any model, but it is necessary to analyze the compressor in its applied environment. The first level in the expanded simulation adds the hermetic motor cooling, the inlet and discharge pressure losses and the discharge pulsation. Figure 8 shows the flowpath in a typical compressor. Losses in the inlet side flow path have several elements — expansion from the inlet line 1, entrance effects from the cavity into the passages through and around the motor (2 and 3), friction in the cooling passages (2 and 3) and expansion into the area ahead of the rotors (4). Additional losses occur as the flow moves around the end of the motor, the bearings and through supports to the rotors. The simulation allows calculation of pressure loss based on a user-defined set of passages (given diameter, length and roughness), expansions and contractions. The program calculates expansion and contraction losses using the appropriate area ratios. Passage losses are computed from pipe friction factors calculated from the well-known Colebrook equation for turbulent regime Reynold's numbers. Figure 9 shows measured suction side pressure loss for a screw compressor run over a wide range of mass flow rates compared to the loss predicted using the model. Modeling of the discharge side pressure losses is carried out in the same fashion, with the added provision for an input loss coefficient for valves (shut-off valves, check valves, etc.).

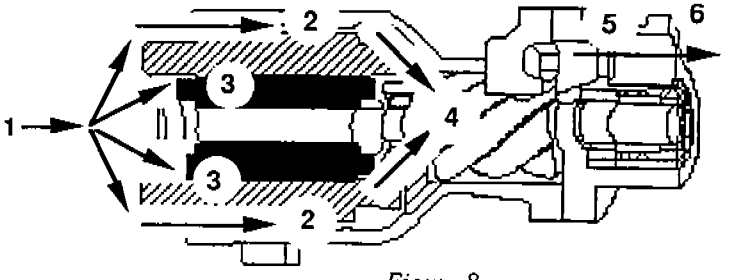

Figure 8
Flow Through Screw Compressor

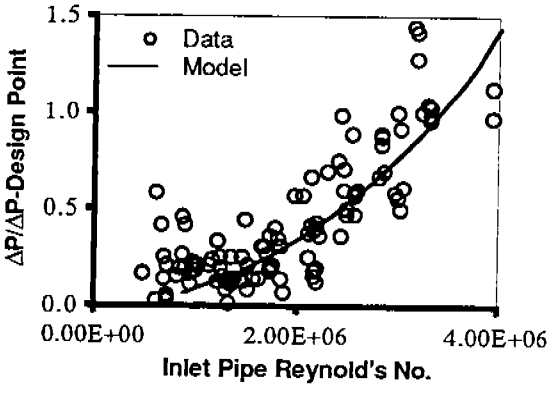

Figure 9
Inlet Side Pressure Loss Characteristics

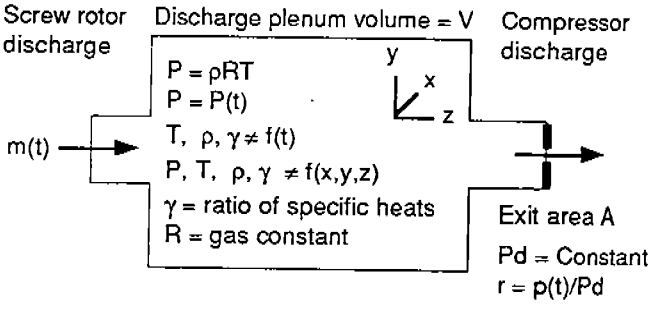

Figure 10
Basis for Simple Pulsation Model

Discharge cavity (location 5 in Figure 8) pressure pulsation is computed using a simple model for a volume V supplied by time-varying mass flow $m(t)$ with a restriction at the discharge represented by an area A and flow coefficient C_d as illustrated in Figure 10. Assuming uniform conditions throughout the volume, using ideal gas relations (for computational speed) and solving for the pressure as a function of time $p(t)$ results in:

$$\frac{dp(t)}{dt} = \frac{RT}{V}\left\{ m(t) - A \cdot C_d \cdot p(t)\sqrt{\frac{2 \cdot \gamma}{(\gamma - 1) \cdot RT}} \cdot \sqrt{r^{2/\gamma} - r^{(\gamma+1)/\gamma}} \right\} \qquad (5)$$

Equation (5) is solved with $m(t)$ from the compression solution, which was arrived at using $p(t)$ from the previous iteration. This simple approach allows the pulsation effect to easily be included in analyses and design optimizations. Solutions for acoustics simulations use separate finite element or boundary element programs, which are not integrated with the performance simulation.

The pressure loss and other auxiliary effects have a strong impact on compressor performance characteristics. The need for good simulations of all of these 'auxiliary' effects is illustrated in Figures 11 and 12. These figures show computed efficiency vs. pressure ratio characteristics for a 127mm, R-22 screw compressor for a variety of built-in volume ratios (Vi). Results in Figure 11 are for computations with no pressure losses on the inlet or discharge sides and no discharge pulsation. These effects are included in the results shown in Figure 12. Figure 12 also shows test results for 2.3 and 2.9 volume ratio compressors. These computations and the tests shown are for constant discharge pressure with varying inlet pressure. Thus, mass flow rates increase as pressure ratio is reduced, accentuating the inlet pressure loss effects. This comparison shows that the inlet and discharge

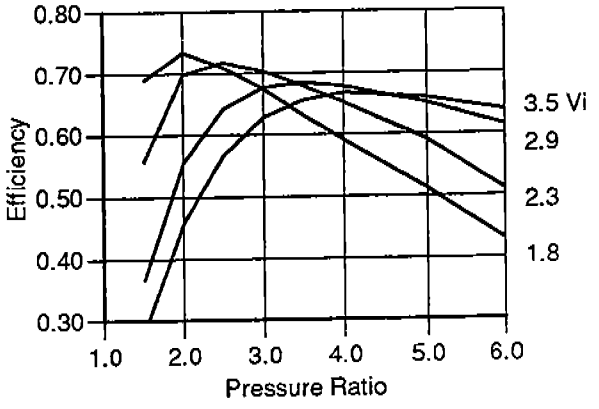

Figure 11
Efficiency Characteristics - Simple Analysis
No Pressure Loss or Pulsation

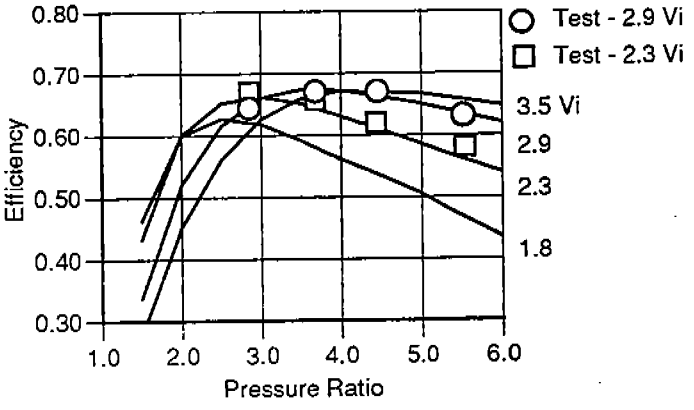

Figure 12
Efficiency Characteristics - Full Simulation
With Pressure Loss and Pulsation

pressure loss and discharge pulsation affect both the performance level and the character of the volume ratio affect. This is especially true at low volume ratios. The simple analysis in Figure 11 shows 1.8 Vi to be the best at pressure ratios below 2.5. However, when the effects of pressure losses and discharge pulsation are added, low Vi offers no advantage at any pressure ratio. The comparisons also show that the benefit of selecting a separate volume ratio for each pressure ratio is less in the applied compressor than when considering the simple analysis characteristics. This effect is most pronounced at lower pressure ratios. The 2.9 Vi is best for pressure ratios from 3.4 to 4.4 in Figure 11. A loss of 4% is seen when 2.9 Vi is used at a pressure ratio of 3. However, in the applied case, the 2.9 Vi option adds no penalty when used at 3:1 pressure ratio and can be applied down to pressure ratios of around 2.5:1 with efficiency penalties less than 4%.

Conclusions

A screw compressor simulation model is described in which a detailed thermodynamic analysis of the compression process in the rotor pair is just part of a comprehensive analysis of the compressor. Numerous design features and application environments can be analyzed with the model. As is often the case, this model relies on relatively simple elemental calculations which are adjusted based on experience or more accurate, separate analyses. Experience has shown us that a careful analysis of clearances greatly improves understanding of test results and leads to more accurate and more broadly applicable calibrations. The general methods for determining the clearances are documented and a brief survey of experimental results showing the measured clearance effects and the results of the model calibration are shown. Finally, the necessity for completeness in compressor simulation is illustrated with an example of the impact of inlet and discharge pressure drop and discharge pulsation.

References

/1/ **Cohen, R.**, Advances in Compressor Technology (as Reported in 1988), *International Journal of Refrigeration*, Vol 13, July 1990.

/2/ **Futakawa, A.**, Improvements in Compressors with Special Emphasis on Interesting Developments in Japan, *Proceedings of the 1984 International Compressor Conference at Purdue*, July 1984.

/3/ **Sauls, J.**, The Influence of Leakage on the Performance of Refrigerant Screw Compressors, *VDI- Berichte 1135 - Schraubenmaschinen '94*, VD Verlag 1994.

/4/ **Peveling, F.**, Ein Beitrag zur Optimierung Adiabater Schraubenmaschinen in Simulationsrechnungen, *Fortschrittberichte VDI, Reihe 7, Strömungstechnik, Nr. 135*, VDI-Verlag 1988.